Impact Modeling of Thermally Sprayed Polymer Particles

Ivosevic, M., Cairncross, R. A., Knight, R., Philadelphia / USA

Thermal spray has traditionally been used for depositing metallic, carbide and ceramic coatings, however, it has recently been found that the high kinetic energy of the High Velocity Oxy-Fuel (HVOF) thermal spray process also enables the solventless processing of high melt viscosity polymers, eliminating the need for harmful, volatile organic solvents. A primarily goal of this work was to develop a knowledge base and improved qualitative understanding of the impact behavior of polymeric particles sprayed by the HVOF combustion spray process. Numerical models of particle acceleration, heating and impact deformation during HVOF spraying of polymer particles have been developed. A Volume-of-Fluid (VoF) computational fluid mechanics package, Flow3D®, was used to model the fluid mechanics and heat transfer during particle impacts with a steel substrate. The radial temperature profiles predicted using particle acceleration and heat transfer models were used as initial conditions in Flow3D® together with a temperature-dependent viscosity model to simulate polymer particles with a low temperature, high viscosity core and high temperature, lower viscosity surface. This approach predicted deformed particles exhibiting a large, nearly hemispherical, core within a thin disk, and was consistent with experimental observations of thermally sprayed splats made using an optical microscope.

1   Introduction

The key advantages of using thermal spray processes for the deposition of polymers include: (i) solventless coating without the use of volatile organic compounds (VOCs); (ii) the ability to coat large objects under almost any environmental conditions; (iii) the ability to apply polymer coatings with high melt viscosity; and (iv) the ability to produce "ready-to-use" coatings without the need for post-deposition processing such as oven drying or curing, typically needed for electrostatic powder coatings and solvent-based paints. The major disadvantages compared to those processes include: (i) lower deposition efficiency, (ii) lower quality surface finish and (iii) higher process complexity, often with a narrow processing window defined by the polymer melting and degradation temperatures.

Three thermal spray processes have reportedly been used for the deposition of polymers [1]:

- Conventional flame spraying.
- HVOF combustion spray.
- Plasma spray.

Only a limited number of polymers sprayed by the HVOF and plasma spray processes have been reported and the commercial applications of HVOF and plasma sprayed polymer coatings are still in the development stage [1]. The HVOF spraying of polymers has gained attention primarily due to the significantly higher particle speeds [up to 1,000 m/s] relative to flame spray [up to ~100 m/s]. This is an important advantage, especially for the deposition of coatings with high melt viscosity, including high molecular weight polymers and polymer/ceramic composites with high (>5 vol.%) ceramic reinforcement contents.

2   Background

The thermal spray unit process is an individual particle or droplet impacting onto a substrate to form a splat. Coating characteristics such as porosity, roughness, adhesive and cohesive strengths depend on the characteristics of these splats and how they bond to the substrate and to each other. As a result, many studies have examined droplet impact behavior in order to understand and improve coating processes [2]. Virtually all of the published modeling of splatting behavior, however, has focused on metallic, ceramic or cermet particles.

One of the principal goals of this work was to develop a knowledge base and improved qualitative understanding of the impact behavior of polymeric particles sprayed by the HVOF combustion spray process. This may not only help to improve understanding of the relationships between processing conditions, coating microstructures and coating properties of HVOF sprayed polymers but also the development of a new low temperature (< 500 °C) thermal spray process capable of efficient and reliable deposition of polymers and polymer/ceramic composites.

As previously reported [3], the large differences in the properties of Nylon 11 and zinc particles resulted in significantly different spreading behavior under similar thermal spray conditions, as may be represented by the Peclet number (Pe). The Pe number for HVOF deposited polymer and metal droplets can be defined as a relative ratio of the droplets' internal heat conduction time ($t_c \sim D^2/\alpha$) and spreading time ($t_s \sim D/V$) scales. Where (D), (V) and (α) are the diameter, impact velocity and thermal diffusivity of a particle. The Pe number of a Zn droplet is in the range 1 - 10 while the Pe number of a Nylon 11 droplet is almost three orders of magnitude larger (Pe ~3,000), indicating that the spreading and cooling of Nylon 11 splats occur over two significantly different time scales. In addition, the substrate can be readily preheated to temperatures at or above the polymer melting temperature. This provides conditions for post-deposition melting of partially melted polymer splats that may enhance their wetting behavior and increase the adhesive strength of the coating. Post-deposition melting of the initial polymer splat layer on

a preheated substrate may provide transition conditions for further coating build-up even if the HVOF sprayed particles are only partially melted.

3 Mathematical Modeling

3.1 HVOF Gas Flow and Thermal Fields

The combustion and exhaust gas characteristics inside the Jet-Kote II® HVOF gun were determined based on calculations carried out by Dobbins et al., 2003 [4] using the same HVOF system as that utilized in this study. The adiabatic flame temperature reported was calculated for a range of combustion chamber pressures and flame stoichiometries defined by a hydrogen-to-oxygen equivalence ratio $\Phi = (H_2/O_2)/(H_2/O_2)_{stoichiometric}$ using Chem-Sage™ thermo-chemical equilibrium software. At the equivalence ratio used in these experiments, $\Phi = 0.83$, the adiabatic flame temperature was ~2,830 ºC at a chamber pressure of 2.2 bar (220 kPa). These conditions, together with the gun internal geometry, were used to estimate a maximum jet velocity of V_g^* ~900 m/s (Mach ~ 0.6).

An empirical correlation [5] for the axial mean velocity (V_g) of the HVOF jet with a range of validity between Mach number 0.3 and 1.4 was used as follows:

$$V_g = V_g^* \left[1 - \exp\left(\frac{\alpha}{1 - \frac{x}{x_c}} \right) \right], \qquad \text{for} \quad x > x_c,$$

$$V_g = V_g^*, \qquad \text{for} \quad x < x_c, \tag{1}$$

where ($\alpha = 0.85$) is the gas velocity decay constant [5], (x) the axial distance along the gun barrel, and (x_c) the jet core length after the gun exit. The jet core length is a function of the nozzle exit diameter (D) and local Mach number (Ma) as defined by the empirical formula (2) [5]:

$$\frac{x_c}{D} = 4.2 + 1.1\,\text{Ma}^2 \tag{2}$$

The water-cooled copper Jet-Kote II® gun nozzle used in this work had a total length of 159.6 mm of which the entry/transition region located between the combustion head and the nozzle itself was only 9.6 mm in length, the remainder (150 mm) was of constant internal diameter (6.35 mm). It was assumed that adiabatic, isentropic and frictionless fluid flow conditions existed within this portion of the gun nozzle with a constant mean velocity and temperature. The mean axial gas temperature had the same functional form as the gas velocity (1) only with a larger

exponential decay exponent ($\alpha = 1.35$) as proposed by Tawfik et al. in 1997 [5].

3.2 Particle Transport

The velocity and temperature of particles during HVOF deposition are the key parameters defining their state and impact conditions and consequently the spreading behavior of impacting droplets. These were computed using momentum and heat transfer equations for particles in the HVOF flow field. It is commonly accepted [6] that the drag force is the dominant force governing the movement of particles in an HVOF jet, so that particle motion can be described by the following two ordinary differential equations:

$$m_p \frac{dV_p}{dt} = \frac{1}{2} C_D \rho_g A_p (V_g - V_p)|V_g - V_p|, \qquad V_p(0) = 0,$$

$$\frac{dx_p}{dt} = V_p, \qquad x_p(0) = 0. \tag{3}$$

where (V_p) is the particle axial velocity, (A_p) the particle projection area, (C_D) the drag coefficient, (ρ_g) the gas density and (x_p) the particle position, calculated from the location where it enters the jet. Note that the relative velocity between particle and gas ($V_g - V_p$) is multiplied to its absolute value, which guaranties that a particle is accelerated in a moving gas if its velocity is lower than the gas velocity and decelerated otherwise. The drag coefficient (C_D) is a function of the Reynolds number [7]:

$$C_D = \left(\frac{24}{\text{Re}} \right) \left(1 + 1.015\,\text{Re}^{0.687} \right), \qquad \text{for Re} < 1000, \tag{4}$$

This correlation was based on the assumption that the particles were spherical, which is consistent with assumptions made in the heat transfer predictions and impact modeling. The Reynolds number for the relative gas flow around a particle of diameter (D_p) is defined as:

$$\text{Re} = \rho_g \frac{|V_g - V_p|}{\mu_g} D_p, \tag{5}$$

where (μ_g) is the dynamic viscosity of the gas.

The Biot number (Bi) of a particle in an HVOF jet gives the ratio of internal and external heat transfer resistances. In other words, for a low Biot number the particles will be heated with negligible internal resistance, resulting in an almost uniform temperature distribution within the particle. This is typically true for most metallic and cermet materials used in thermal spraying (Bi < 0.1) and has led to a number of authors [4, 8-9] neglecting temperature gradients within the particles. In the case of polymers, the Biot number for a particle in an HVOF jet is typically much higher (Bi >

5) implying that the most of particles are likely to develop large temperature gradients between the core and the surface. Accordingly, the equation describing the heat transfer from the gas to a single spherical particle in spherical coordinates with appropriate initial and boundary conditions is of the form:

$$\rho_p Cp \frac{\partial T_p}{\partial t} = \frac{1}{r^2} \frac{\partial}{\partial r}\left(r^2 k_p \frac{\partial T_p}{\partial r}\right), \qquad (6)$$

$$T_p(r, t = 0) = T_p^o$$

$$\frac{dT_p}{dr}(r = 0) = 0, \qquad -k_p \frac{dT_p}{dr}(r = R) = h\left(T_{p(R)} - T_g\right),$$

where (T_p) is the particle temperature, and (ρ_p), (Cp), and (k_p) are the density, heat capacity and thermal conductivity of the particle, and (r) is a parameter which represents the current particle diameter taking values between (0) and the overall particle diameter (R).

The equations for momentum and heat transfer were solved by numerical integration using the Forward Euler method with a time step small enough $(10^{-7}$ s$)$ that the local Reynolds number, gas velocity and temperature could be considered constant over each time step.

3.3 Particle Impact

A "Volume of Fluid" (VoF) method, developed by Hirt and Nichols [10], namely FLOW-3D® (version 9.0) was chosen to study the fluid mechanics and heat transfer during particle impact with a substrate because of the complex three-dimensional morphology of "splats" formed during thermal spraying. The initial impact conditions of an HVOF sprayed particle, such as particle impact velocity and internal temperature profile, were incorporated into the FLOW-3D® model from the momentum and heat transfer predictions, as described earlier.

Molten Nylon 11 was modeled as a viscous shear thinning fluid with a temperature dependent viscosity using a Carreau model [11] in the form:

$$\mu = \mu_\infty + \frac{\mu_0 - \mu_\infty}{\left(1 + \lambda^2 \dot{\gamma}^2\right)^{\frac{1-n}{2}}}, \qquad (7)$$

where (μ) is the polymer dynamic viscosity, $(\mu_\infty = 0)$ and $(\mu_o = 13{,}000$ Poise at T = 220 ºC$)$ are infinite shear-rate and zero shear-rate viscosities, respectively, $(\lambda = 1)$ is a time constant, $(n = 0.7)$ is the "power-low exponent," and $(\dot{\gamma} = 0.001 - 10{,}000$ s$^{-1})$ is the polymer shear rate. All coefficients were determined based on experimental measurements on Nylon 11 material using the cone & plate method, and the zero-shear-rate viscosity is a temperature-

dependent parameter. These results will be reported separately.

4   Experiments

A semicrystalline Polyamide (Nylon 11) powder commercially available as Rilsan PA-11 French Natural ES D-60 (donated by Arkema) was used as the feedstock material in this work. As-received powder had a mean particle size of 60 µm and corresponding particle size distribution of -102/+26 µm. The melting and degradation temperatures of Nylon 11, as reported by the manufacturer, were in the range 182 - 191 ºC and 357 - 557 ºC, respectively. Swipe or "splat" tests involving single high speed [> 0.7 m/s] spray passes across room temperature glass slides at low powder feed rates [~2 g/min] were used to observe the morphology of individual splats. In addition, Nylon 11 particles were also deposited on a substrate preheated to 200 °C in order to further understand the influence of substrate preheating on the deposition behavior of the Nylon 11 material. Splat tests were carried out using the Stellite Coatings, Inc. Jet-Kote II® HVOF spray system using an O_2/H_2 ratio of 0.0024/0.0039 m^3/s (300/500 scfh) and spray distance of 200 mm. Splat morphologies sprayed both with and without substrate preheating were analyzed using standard optical microscopy with polarized light (Olympus PMG-3 optical metallograph).

In-flight particle velocities at a distance of 100 mm from the nozzle exit were measured using the *SprayWatch 2i* system in conjunction with a diode laser illumination source, both provided by Oseir Ltd. from Tampere, Finland. The particle velocities were measured for four (4) different spray conditions varying the total gas flow rate at a constant oxygen: hydrogen ratio ($\Phi = 0.83$). The four total gas flow rates used were 1.86, 2.23, 2.61 and 2.98 g/s. The typical number of particles analyzed was in the range 200 - 300 in all four cases.

5   Results and Discussion

Most of the larger Nylon 11 splats sprayed onto a room temperature substrate exhibited a characteristic "fried-egg" shape with a large nearly-hemispherical core in the center of a thin disk (**Fig. 1**). This shape indicated the existence of a large radial difference in flow properties of the molten or nearly molten nylon droplets and largely unmelted core. In other words, the "fried-egg" shaped splats were formed by polymer particles having a large radial temperature profile – a low temperature, high viscosity core and a high temperature, low viscosity surface.

On the other hand, nylon splats sprayed onto a preheated substrate exhibited a flattened hemispherical shape (**Fig. 2**) likely due to post-deposition flow activated by surface tension or/and residual stress after the initially "fried-egg" morphology splats were fully melted by the preheated substrate (**Fig. 3**). It was observed that post-deposition flow of Nylon 11 splats occurred only when

the substrate was preheated to temperatures above ~185 °C, which was consistent with the onset of melting of nylon's crystalline phase.
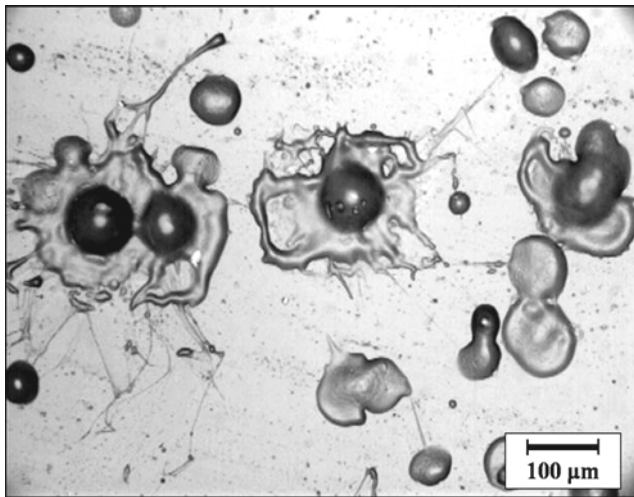
Fig. 1. Nylon 11 splats deposited onto a room temperature glass slide.
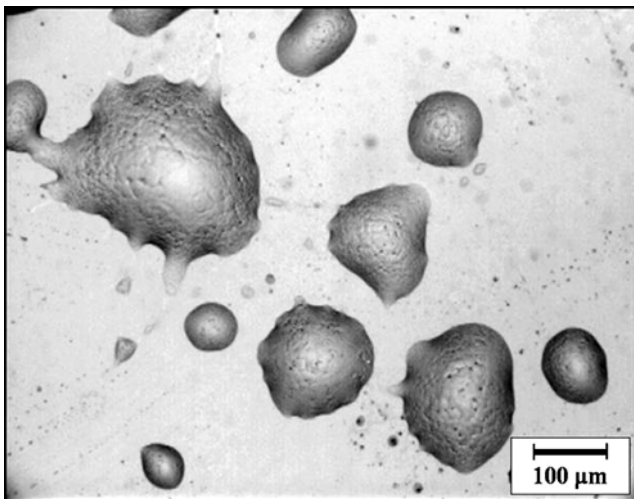
Fig. 2. Nylon 11 splats deposited onto a preheated glass slide (200 °C).
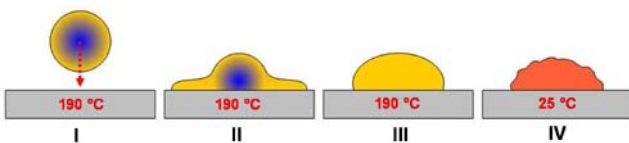
Fig. 3. Nylon 11 impact sequence onto a preheated substrate, (I) partially melted particle before impact, (II) "fried-egg" shaped splat, (III) post-deposition flow of a fully molten droplet, (IV) droplet shrinkage during cooling.

The results of in-flight particle velocity measurements using the *SprayWatch 2i* system are shown in **Fig. 4**. Mean particle velocities of 433, 479, 546 and 563 m/s were measured for the four gas flow rates investigated. Note that the highest O_2 + H_2 gas flow rate of 480 + 800 scfh (a total gas mass flow rate of 2.98 g/s at $\Phi = 0.83$) did not follow the same trend of particle velocity increase as was observed for the other three spray conditions. The highest O_2 + H_2 gas flow rates used in this experiment were the only spray conditions corresponding to a sonic (~Mach 1) jet velocity, characterized by the appearance of expansion and compression pressure waves ("shock diamonds"). It was believed that the lower mean particle velocity produced at the highest O_2 + H_2 gas flow rate was the result of polymer particle interactions with the shock structure.
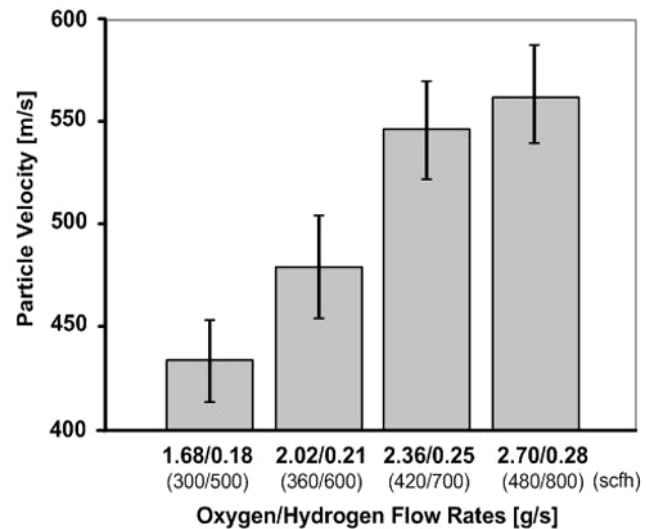
Fig. 4. In-flight Nylon 11 particle velocity as a function of O_2 + H_2 gas flow rate.

The predicted Nylon 11 particle velocities as a function of particle size are shown in **Fig. 5**. In general, polymer particles accelerated much faster relative to metallic or cermet particles in HVOF jets [4, 9]. This was due to the similar size but much lower densities of polymers (0.9 - 1.4 g/cm^3) versus metals or cermets (2.7 - 15 g/cm^3). For the same reason, however, the polymer particles will have lower inertia and their velocity will decay faster as they exit the gun nozzle than metals and cermets. One possible way to maximize the impact velocity of polymer particles would be to reduce the spray distance. This approach, however, has limited potential due to the potentially destructive effect of the HVOF jet on polymeric coatings at low gun surface speeds [12]. The predicted particle velocity of 700 m/s for 60 μm particles at a 100 mm spray distance was significantly higher than the experimentally measured particle velocity (410 - 450 m/s). This indicated that the gas flow and particle acceleration models used require further optimization to provide improved agreement with experimental measurements.

The heat transfer from the combusting gas to Nylon 11 particles was computed using the residence time of particles in the HVOF jet based on the predicted particle velocity and the spray distance (**Fig. 5**). Predicted temperature profiles within the Nylon 11 particles at a spray distance of 200 mm (8 in) at the

moment of impact with the substrate are shown in **Fig. 6**. These predictions were qualitatively consistent with the experimental observations of Nylon 11 splats sprayed onto a room temperature substrate. Larger particles (>45 μm) had unmelted or partially melted cores, which likely resulted in the formation of the "fried-egg" shape splats observed.
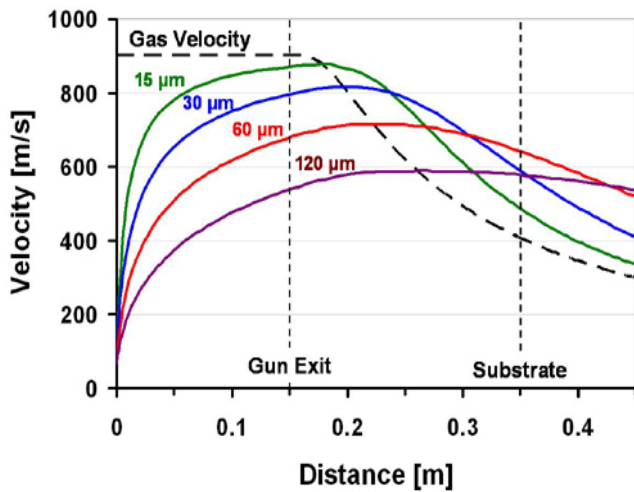
Fig. 5. Predicted velocities of Nylon 11 particles in an HVOF jet (total $O_2 + H_2$ gas flow rate of 1.86 g/s at $\Phi = 0.83$).
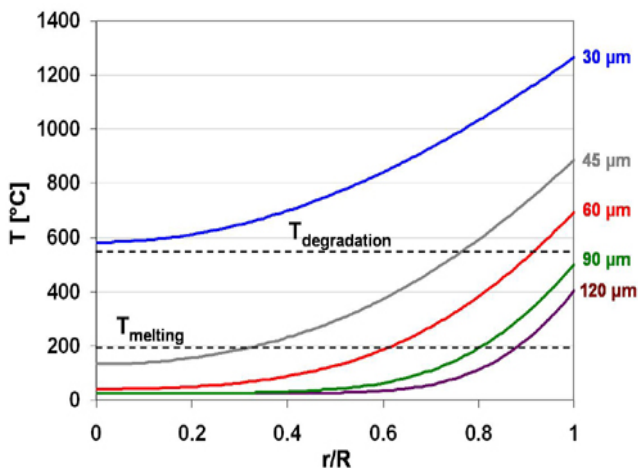
Fig. 6. Predicted temperature profiles within Nylon 11 particles immediately before impact with a substrate at 200 mm spray distance.

The radial temperature profiles predicted using the particle acceleration and heat transfer models were used as the initial conditions in Flow3D® for a temperature-dependent Carreau viscosity model. This generated particles with a low temperature (high viscosity) core and high temperature (low viscosity) surface. The predicted shapes of deformed particles exhibited a large nearly-hemispherical core in the center of a thin disk, which was consistent with experimental observations of HVOF sprayed splats (**Fig. 7**). Improvement of the model to include multiple particle impacts and modeling of the post-deposition

flow of nylon splats on a preheated substrate is in progress and will be reported separately.
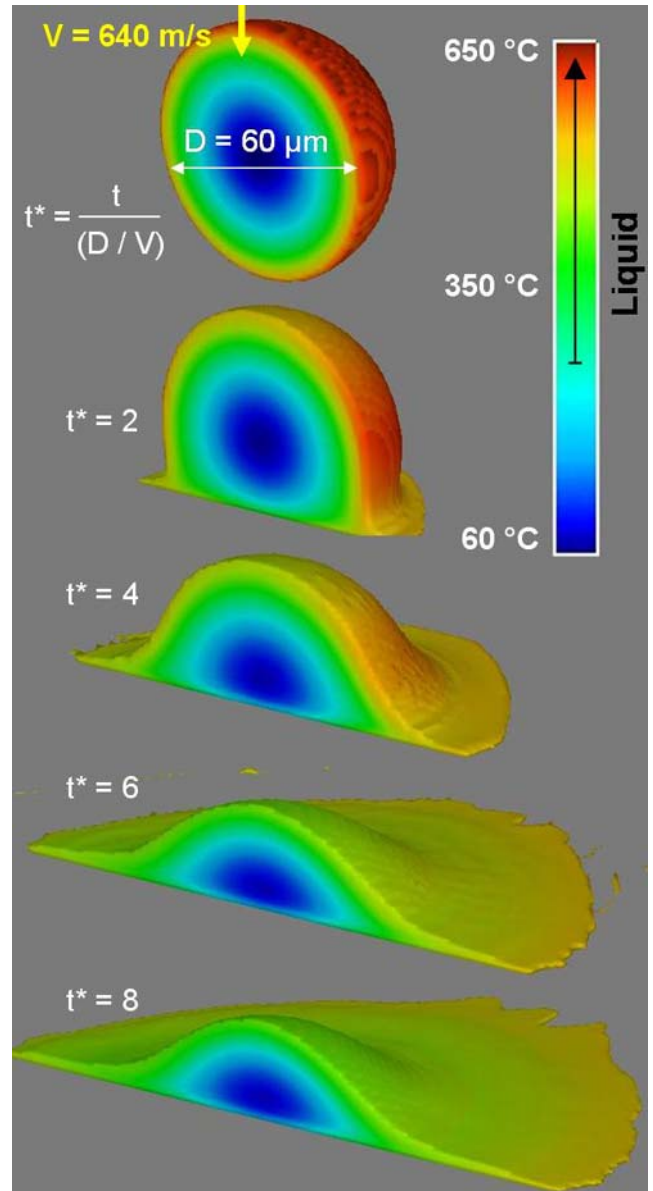
Fig. 7. Simulated deformation of a Nylon 11 droplet with a radial temperature gradient and temperature-dependent viscosity during impact.

6   Summary and Conclusions

One of the principal goals of this work was to develop a knowledge base and improved qualitative understanding of the impact behavior of polymeric particles sprayed by the HVOF combustion spray process. Mathematical models of particle acceleration, heating and impact of Nylon 11 particles have been developed. In general, polymer particles accelerated and decelerated much faster than metallic and cermet particles of similar size due to the much lower density of polymers. In addition, the high Biot number (Bi > 5) for polymer particles in an HVOF jet relative to metals indicated that most of the particles would likely develop a steep temperature gradient

between the particle core and its surface. This was consistent with experimental observations of thermally sprayed splats, since most of the Nylon 11 splats sprayed onto a room temperature substrate exhibited a "fried-egg" shape with a large nearly-hemispherical core in the center of a thin disk.

The radial temperature profiles predicted using particle acceleration and heat transfer models were used as initial conditions in Flow3D$^{®}$ with a temperature-dependent Carreau viscosity model; this generated particles with a low temperature (high viscosity) core and high temperature (low viscosity) surface. The predicted shapes of deformed particles also exhibited good qualitative agreement with experimentally observed "fried-egg" shape splats.

7   Acknowledgements

8   References

[1] Petrovicova, E. and Schadler L. S., "Thermal Spray of Polymers," International Materials Reviews, Vol. 47 (4), pp. 169-190, (2002).

[2] Fauchais, P., Fukomoto, M., Vardelle, A. and Vardelle, M., "Knowledge Concerning Splat Formation: An Invited Review," Journal of Thermal Spray Technology, 13 (3), pp. 337 - 360, (2004).

[3] Ivosevic, M., Cairncross, R. A. and Knight, R., "Heating and Impact Modeling of HVOF Sprayed Polymer Particles," Proc. 2004 International Thermal Spray Conference [ITSC-2004], DVS/IIW/ASM-TSS, Osaka, Japan, May 10-12, (2004).

[4] Dobbins, T. A., Knight, R. and Mayo, M. J., "HVOF Thermal Spray Deposited Y_2O_3-Stabilized ZrO_2 Coatings for Thermal Barrier Applications," Journal of Thermal Spray Technology, 12 (2), pp. 214 - 225, (2003).

[5] Tawfik, H. H. and Zimmerman, F., "Mathematical Modeling of the Gas and Powder Flow in HVOF Systems," Journal of Thermal Spray Technology, 6 (3), pp.345 - 352, (1997).

[6] Cheng, D., Trapaga, G., McKelling, J. W. and Lavernia, J. E., "Mathematical Modeling of High Velocity Oxygen Fuel Thermal Spraying: An Overview," Key Engineering Materials, 197, pp.1 -26, (2001).

[7] Yang, X. and Eidelman, S., "Numerical Analysis of a High-Velocity Oxygen-Fuel Thermal Spray System," Journal of Thermal Spray Technology, 5 (2), pp.175 - 184, (1996).

[8] Pasandideh-Fard, M., Parshin, V., Chandra, S., and Mostaghimi, J., "Splat Shapes in a Thermal Spray Coating Process: Simulations and Experiments," Journal of Thermal Spray Technology, 11 (2), pp. 206 - 217, (2002).

[9] Li, M. and P. D. Christofides, "Feedback Control of HVOF Thermal Spray Process Accounting for Powder Size Distribution," Journal of Thermal Spray Technology, 13 (1), pp.108 - 120, (2004).

[10] Hirt, C. W. and Nichols, B. D., "Volume of Fluid (VoF) Method for the Dynamics of Free Boundaries," J. of Computational Physics, 39, pp. 201 - 225, (1981).

[11] Macosko, C. W., "Rheology - Principles, Measurements and Applications," Wiley-VCH, Inc., (1994).

[12] Gawne D. T., Zhang T. and Bao Y., "Heating Effect of Flame Impingement on Polymer Coatings," Proc. ITSC 2001, Eds. Berndt, C. C, Khor, K. A. and Lugscheider, E. F., Singapore, ASM International®, Materials Park, OH, pp. 307-313, (2001).